Electronic Supplementary Material (ESI) for Journal of Materials Chemistry A.
This journal is © The Royal Society of Chemistry 2020

Enhancing the Performance of Supercapacitors through Constructing "Mini Parallel-Plate Capacitor" in Electrode with High Dielectric Constant Materials

Huayao Tu,[a] Shouzhi Wang,[a] Hehe Jiang,[a] Zhenyan Liang,[a] Dong Shi,[a] Yongliang Shao,[a,b] Jianxing Shen,[b] Yongzhong Wu[a,b] and Xiaopeng Hao*[a,b]*

[a] State Key Lab of Crystal Materials, Shandong University, Jinan, 250100, P.R. China

[b] Department of Materials Science and Engineering, Qilu University of Technology, Jinan, 250353, P. R. China.

*E-mail: wuyz@sdu.edu.cn; xphao@sdu.edu.cn

S1. Chemicals

$FeCl_3 \cdot 6H_2O$, V_2O_5, $SnCl_4 \cdot 5H_2O$, tetrabutyl titanate (TBT), Urea, SDS, CTAB, HCl, ethylene glycol (EG), KOH, H_2O_2, NaBr, $H_2C_2O_4$ and ethanol were purchased from Sinopharm Chemical Reagent Co., Ltd. (Shanghai). All those reagents were analytical grade. NH_3, N_2 purchased from Deyang special Gas Co., Ltd. (Jinan, China).

S2. Synthetic Methods

Preparation of acid treated carbon fiber: In a typical procedure, a piece of carbon fiber cloth (1.5 cm× 4cm) was subsequently cleaned with DI water and ethanol under ultrasonic, and dried in an oven. Then, the freshly cleaned CF was added into a stainless-steel autoclave (100mL) containing commercially available concentrated HNO_3 (50 mL) and DI water (15 mL), and was hold at 120 °C for 12 h. Then, the resulted CF was washed thoroughly with DI water until the pH is close to 7.

Synthesis of FeO_xN_y nanorods: a Teflonlined stainless-steel autoclave with a capacity of 50 mL was filled with 30 mL of an aqueous solution containing 0.4 g ferric chloride ($FeCl_3 \cdot 6H_2O$), 0.2 g urea, and 0.02 g sodium lauryl sulfate (SDS). A 1.5 cm × 4 cm piece of clean carbon fiber treated with air plasma was immersed in the precursor solution in an autoclave. The autoclave was heated at 100 °C for 12 h and then cooled to room temperature. Hydroxides grown on the carbon fiber were washed with deionized water and ethanol and dried at 60 °C in air. The asprepared FeOOH samples were further thermally annealed at 350 °C under NH_3 atmosphere for 2 h at the heating rate of 2 °C min^{-1}. For comparison, the Fe_2O_3 samples was obtained by annealed at 350 °C under nitrogen (N_2) atmosphere for 2 h. Powder samples of Fe_2O_3 were prepared by the same method.

Synthesis of VO_xN_y nanorods: first, 0.9 g of V_2O_5 powder and 1.35 g of $H_2C_2O_4$ powder were dissolved with 30 mL of distilled water at 75 °C for 12h. 10 ml of the above solution was transferred into a 50 mL Teflon lined stainless steel autoclave. Then 1 mL of 30% H_2O_2 and 20 mL of ethanol were added and kept continuously stirring for about 30 min; then, one piece of acid treated clean carbon fiber (1.5 cm × 4 cm) was immersed into the reaction solution. The autoclave liners were kept at 180 °C for 3 h and then the sample was collected and rinsed with ethanol and distilled water. The obtained hydroxide array growth on the carbon cloth was washed with deionized (DI) water, ethanol and dried at 60 °C. Following the as-prepared samples were further thermally annealed at 550 °C under ammonia (NH_3) atmosphere for 1 h with the heating rate of 3°C min^{-1}, during the heating and cooling process use N_2 atmosphere protection.

For comparison, the VO_2 samples was obtained by annealed at 550°C under nitrogen (N_2) atmosphere for 2 h. Powder samples of VO_2 were prepared by the same method.

Synthesis of SnO_xN_y nanorods: first, 0.927 g of NaBr powder were dissolved with 3 mL of distilled water in beaker A and stirred 0.5 hour. Identically, 0.1 g of $SnCl_4 \cdot 5H_2O$ were dissolved with 20 mL of glacial acetic acid in beaker B and stirred 0.5 hour. Then, the solution in beaker A and beaker B was mixed and stirred for 0.5 hour to form mixed solution. After that, the above solution was transferred into a 50 mL Teflon lined stainless steel autoclave and 3 mL of ethanol (Et) were added and kept continuously stirring for about 0.5 hour; then, one piece of acid treated clean carbon fiber (1.5 cm × 4 cm) was immersed into the reaction solution. The autoclave liners was kept at 200 °C for 24 h and then the obtained hydroxide array growth on the carbon fiber was washed with deionized (DI) water, ethanol and dried at 60°C. Following the as-prepared samples were further thermally annealed at 475°C under ammonia (NH_3) atmosphere for 4 h with the heating rate of 3 °C min^{-1}, during the heating and cooling process use N_2 atmosphere protection. For comparison, the SnO_2 samples was obtained by annealed at 475 °C under nitrogen (N_2) atmosphere for 4 h. Powder samples of SnO_2 were prepared by the same method.

S3. Materials Characterization

The morphology and phase structure of the samples were investigated with FESEM (Hitachis-4800), HRTEM (JEM 2100F), XRD (Bruker D8 Advance), XPS (Philips Tecnai Twin-20U), and Raman (Horiba Jobin Yvon), respectively.

S4. Electrochemical Tests

The electrochemical characterizations of the CM and the CMM were tested using a three-electrode system on a CHI660E electrochemical workstation (Shanghai Chen Hua Instruments Co., China). In the test system, the self-supported binder-free CM and CMM were used as the work electrode, with a platinum sheet (2 cm × 2 cm) as a counter electrode and Hg/HgO as a reference electrode, in 6.0 M KOH aqueous solution.

All the electrochemical measurements with galvanostatic charge/discharge (GCD), cyclic voltammetry (CV), and electrochemical impedance spectroscopy (EIS) techniques were conducted in three-electrode system. For detail, CV and GCD curves were collected at –1 V to 0 V against Hg/HgO by varying the scan rate from 5 mV s^{-1} to 100 mV s^{-1} and current density from 0.1 A g^{-1} to 10 A g^{-1}, respectively. Alternating current EIS spectra were collected within a frequency range of 10^{-2} Hz – 10^{5} Hz at the open circuit voltage with AC amplitude of 5 mV.

For three-electrode cells, specific capacity derived from GCD discharge curves was calculated as:

$$C(F/g) = I\int (1/V(t))dt$$

where I is the applied constant-current density, t is the discharge time, and V(t) is the potential as a function of t.

Dielectric constant test of metal oxide materials: The metal oxide powder of the corresponding crystal type and morphology is pressed into a small wafer with an area of 1.37 mm^2 and a certain thickness (0.75~1.37 mm) by a tablet press, and its capacitance and dielectric loss are measured by Impedance analyzer (Agilent-4294A).

Then, the dielectric constant of the metal oxide is obtained from the measured capacitance.

S5. Supplementary Figures S1–S19

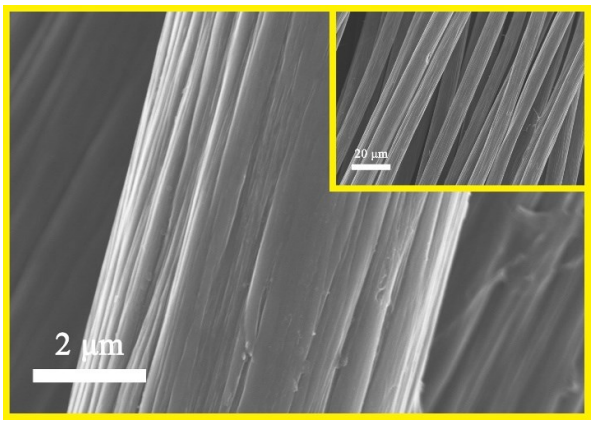

Figure S1. SEM image of acid treated clean carbon fiber.

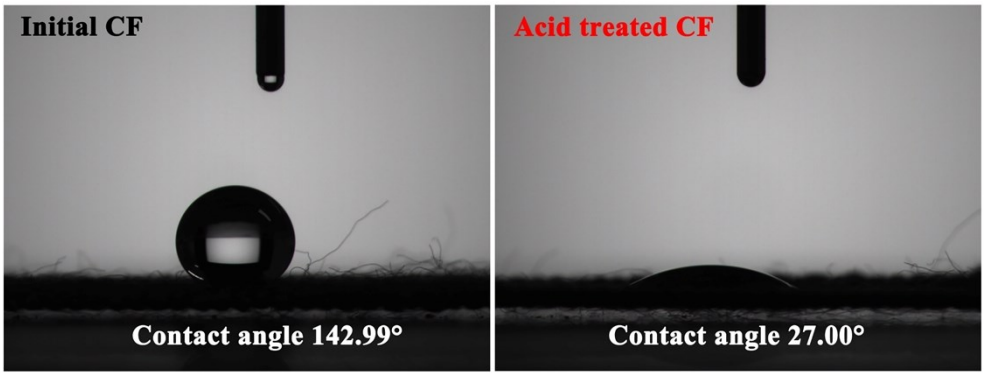

Figure S2. Water contact angles of CF and acid treated clean CF.

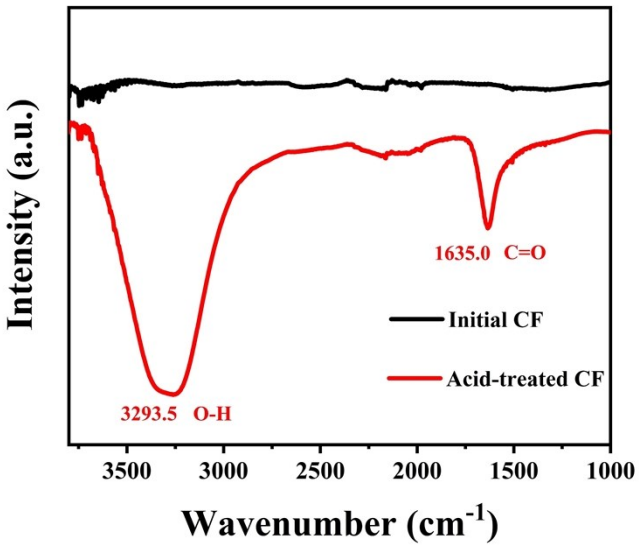

Figure S3. Fourier transform infrared spectroscopy (FTIR) spectra of CF and acid treated clean CF.

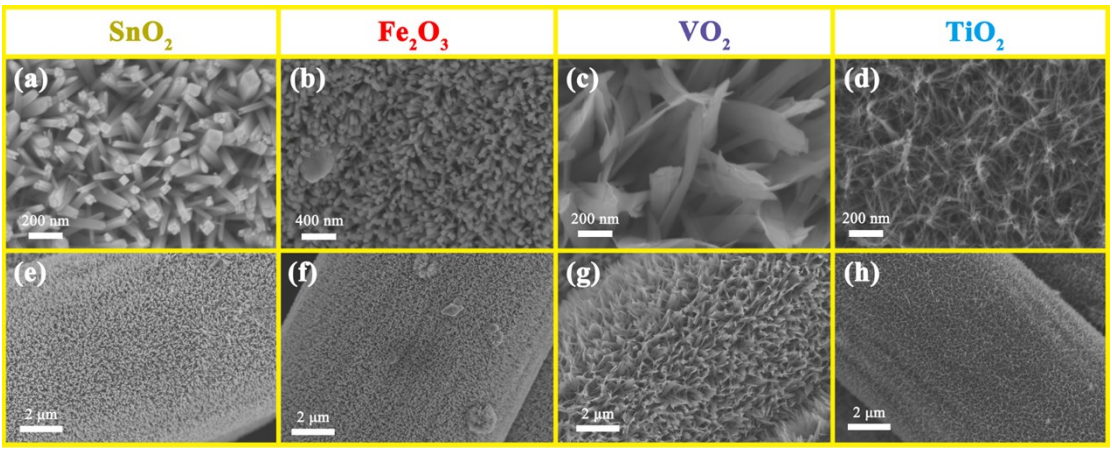

Figure S4. SEM images of the corresponding (a, e) SnO_2, (b, f) Fe_2O_3, (c, g) VO_2 and TiO_2 (d, h) hydroxide precursors used for preparing metal oxynitride nanorods at different magnification.

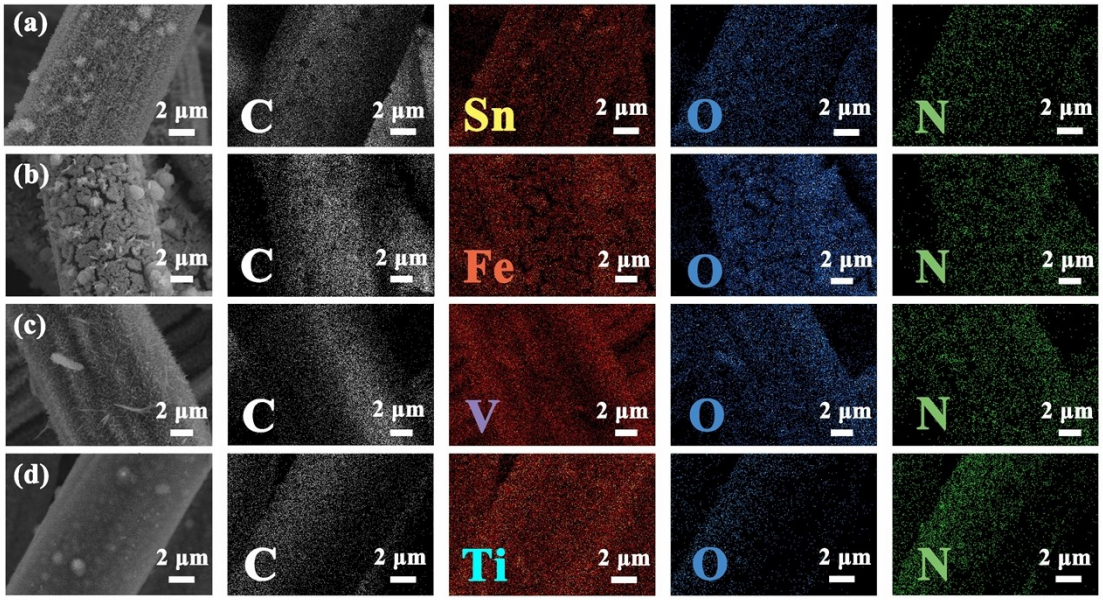

Figure S5. Elemental mapping images of the as-prepared SnO_xN_y (a), FeO_xN_y (b), VO_xN_y (c) and TiO_xN_y (d) samples.

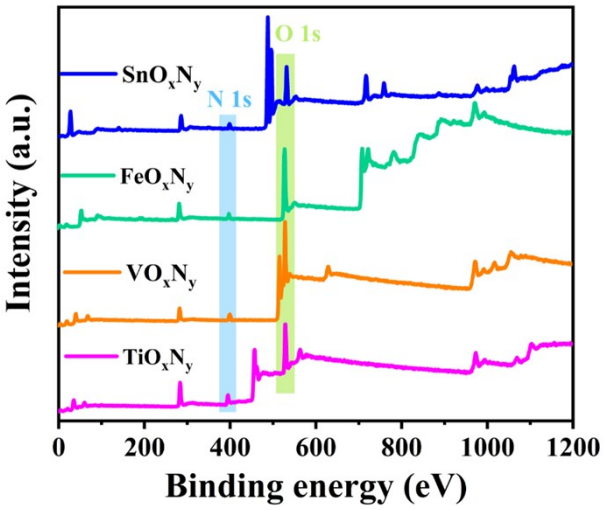

Figure S6. The XPS spectra of survey spectra.

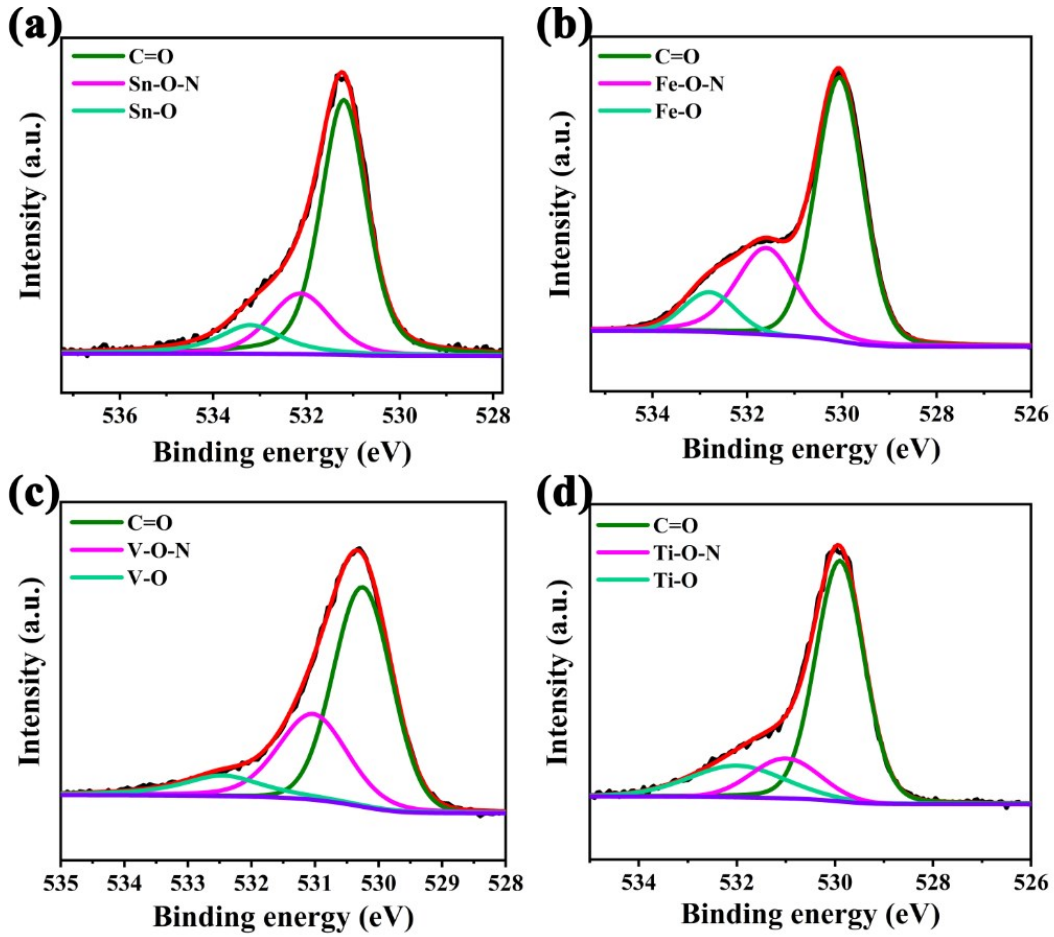

Figure S7. Corresponding high-resolution O 1s spectra of SnO_xN_y (a), FeO_xN_y (b), VO_xN_y (c) and TiO_xN_y (d), respectively.

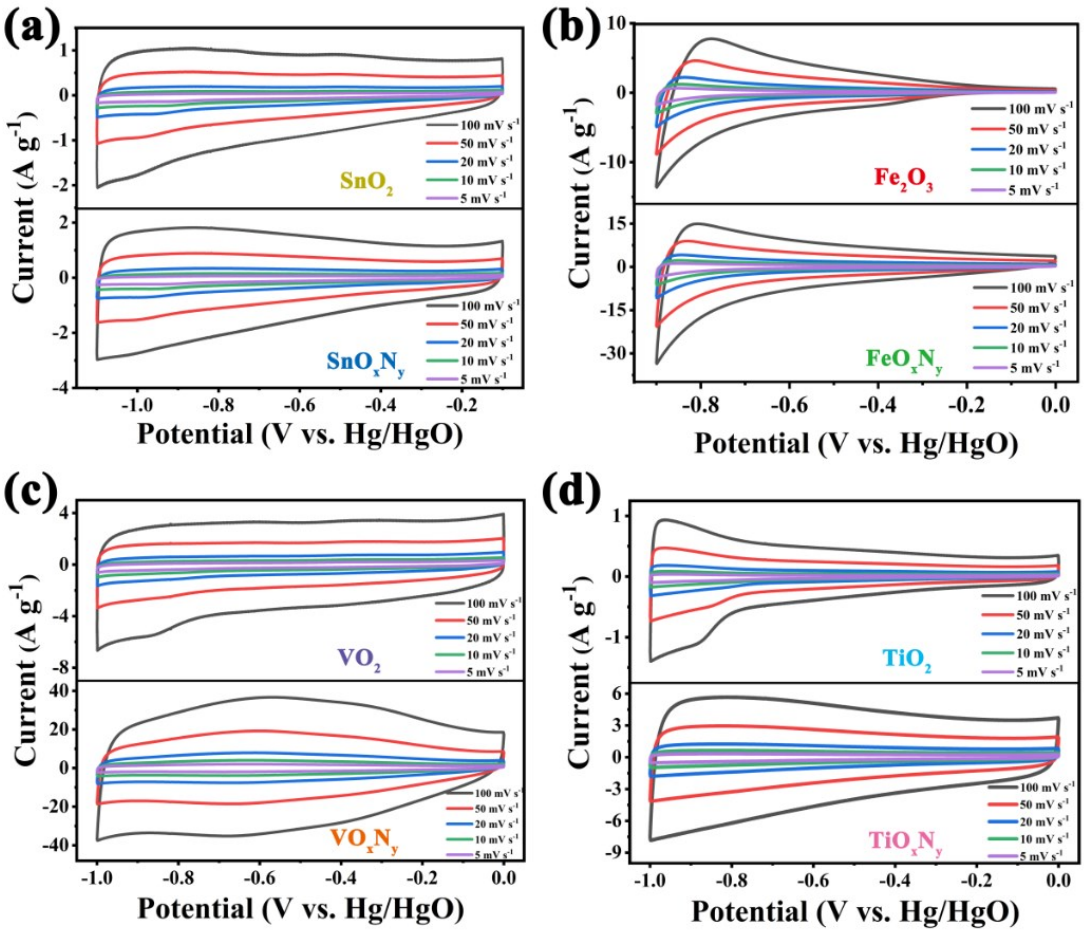

Figure S8. The CV curves at increasing scan rates of the SnO_2 and SnO_xN_y (a), Fe_2O_3 and FeO_xN_y (b), VO_2 and VO_xN_y (c), TiO_2 and TiO_xN_y (d) electrodes.

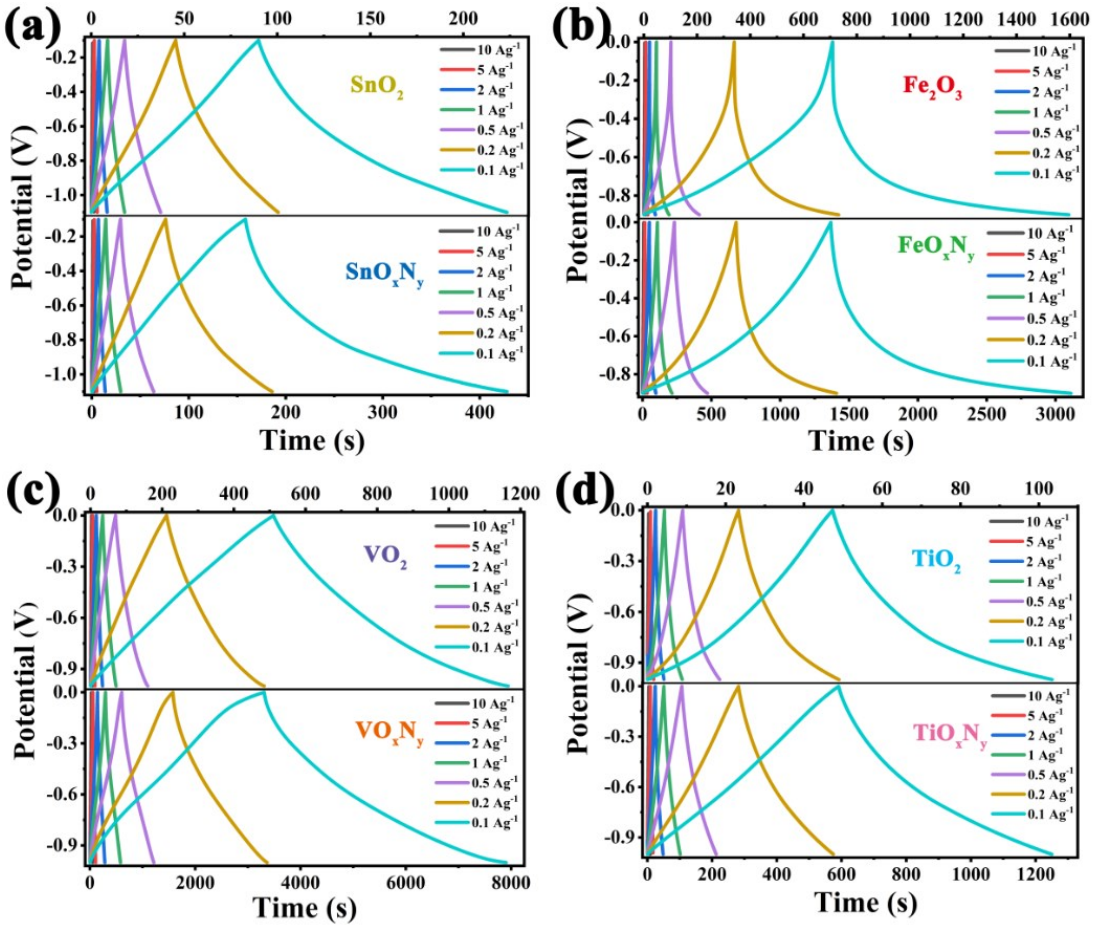

Figure S9. The GCD curves at increasing current density of the SnO_2 and SnO_xN_y (a), Fe_2O_3 and FeO_xN_y (b), VO_2 and VO_xN_y (c), TiO_2 and TiO_xN_y (d) electrodes.

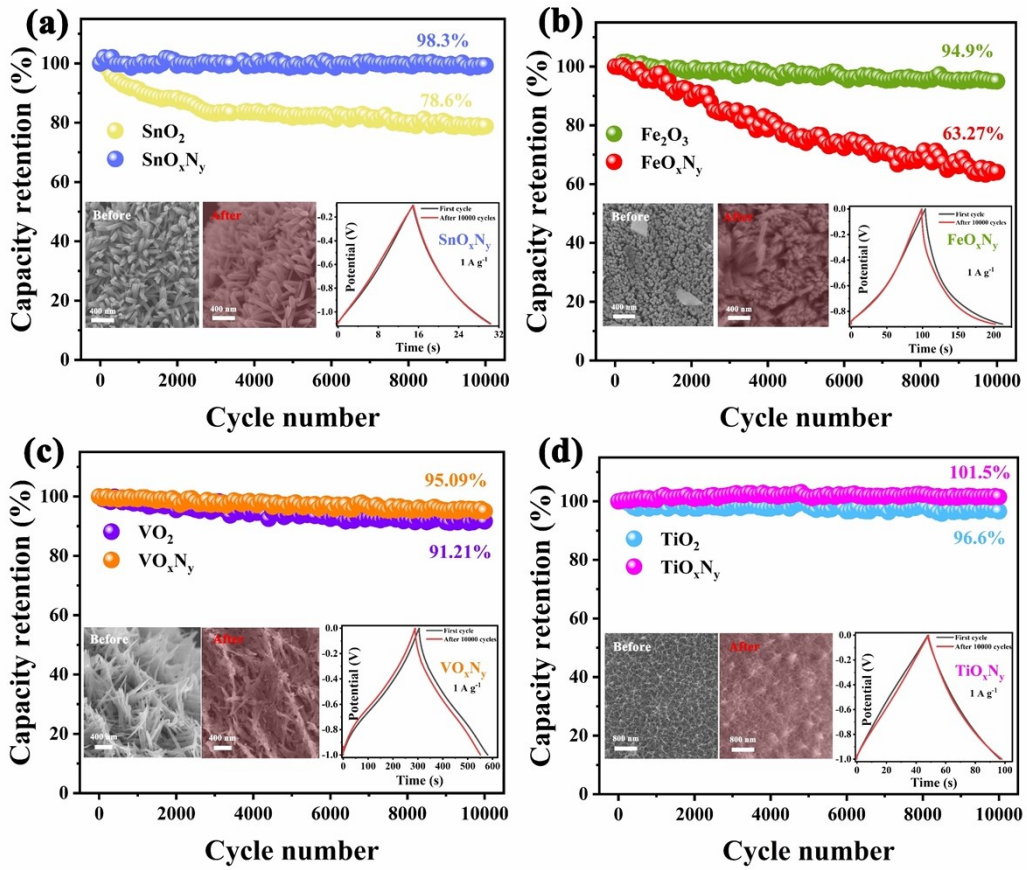

Figure S10. Charge/discharge cycling performance of CM electrodes and CMM electrodes, insets figures are SEM images and GCD curves before and after 10000 cycles.

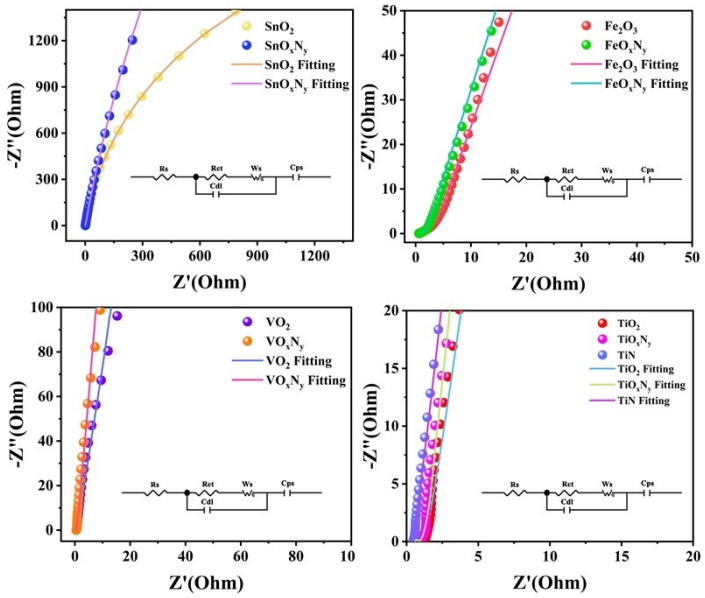

Figure S11. Nyquist plots of the electrodes, with inset showing the equivalent circuit model.

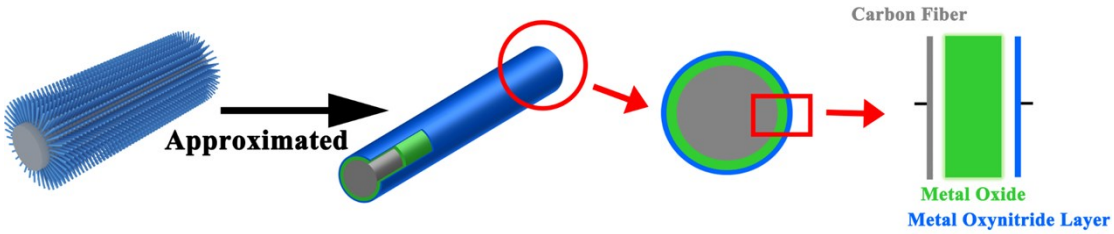

Figure S12. Metal oxynitride nanorods on each carbon fiber can be approximated to a coaxial mini parallel-plate capacitor, form a sandwich structure.

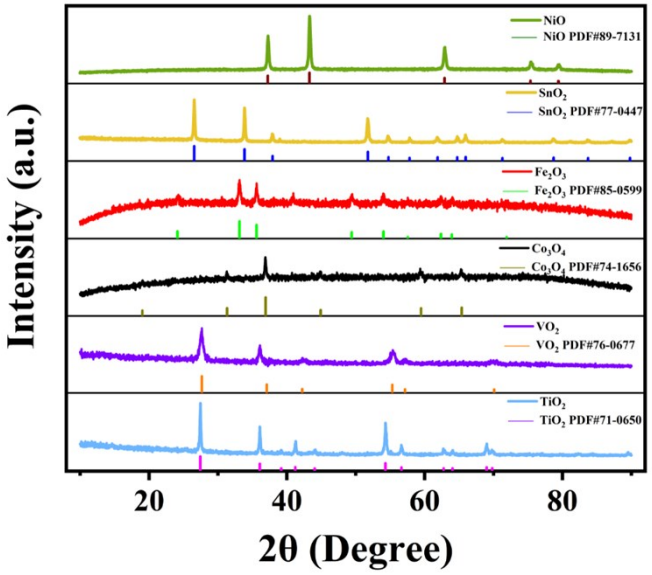

Figure S13. XRD patterns of the metal oxides powder.

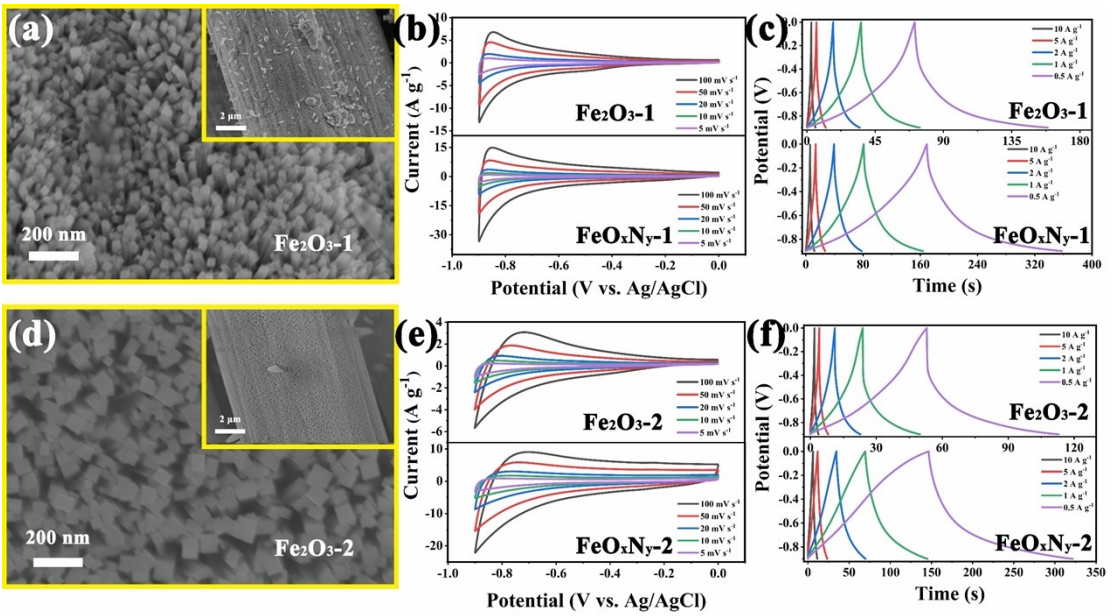

Figure S14. (a) SEM images of Fe_2O_3-1 (small 'A' value); (b) CV curves of Fe_2O_3-1 and FeO_xN_y-1; (c) GCD curves of Fe_2O_3-1 and FeO_xN_y-1; (d) SEM images of Fe_2O_3-2 (large 'A' value); (e) CV curves of Fe_2O_3-2 and FeO_xN_y-2; (f) GCD curves of Fe_2O_3-2 and FeO_xN_y-2.

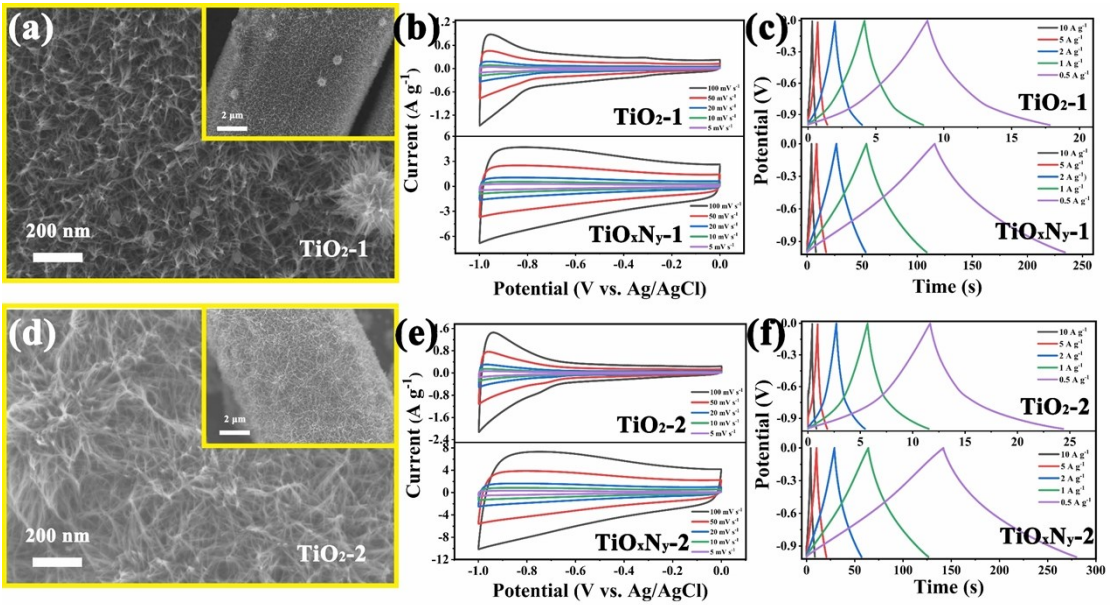

Figure S15. (a) SEM images of TiO_2-1 (small 'd' value); (b) CV curves of TiO_2-1 and TiO_xN_y-1; (c) GCD curves of TiO_2-1 and TiO_xN_y-1; (d) SEM images of TiO_2-2 (large

'd' value); (e) CV curves of TiO_2-2 and TiO_xN_y-2; (f) GCD curves of TiO_2-2 and TiO_xN_y-2.

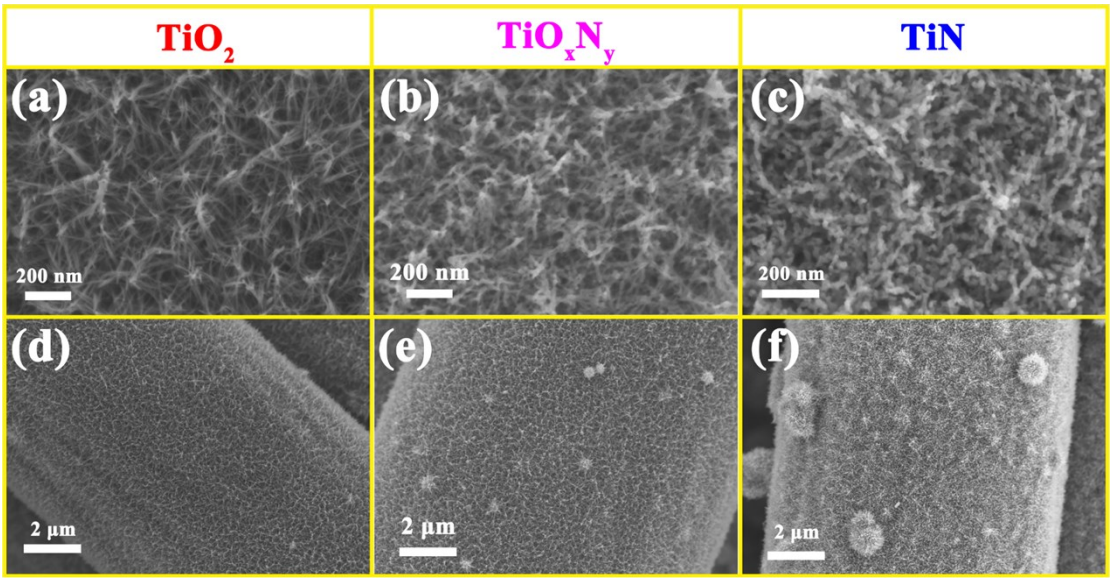

Figure S16. SEM images of the corresponding (a, d) TiO_2, (b, e) TiO_xN_y, (c, f) TiN at different magnification.

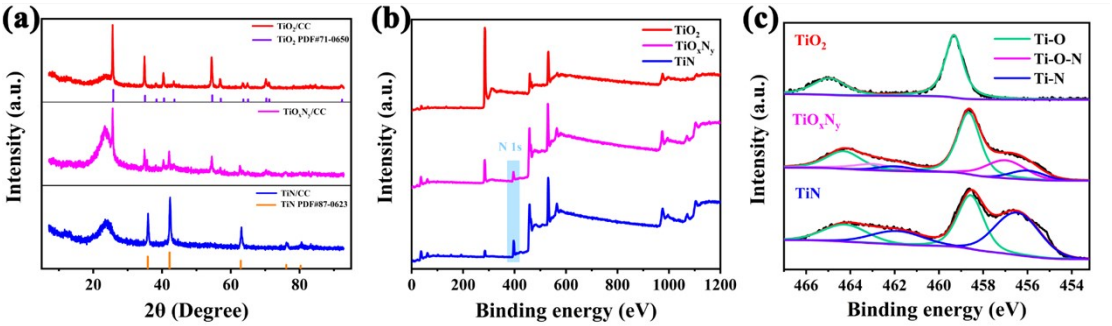

Figure S17. XRD patterns and XPS spectra of the TiO_2, TiO_xN_y and TiN.

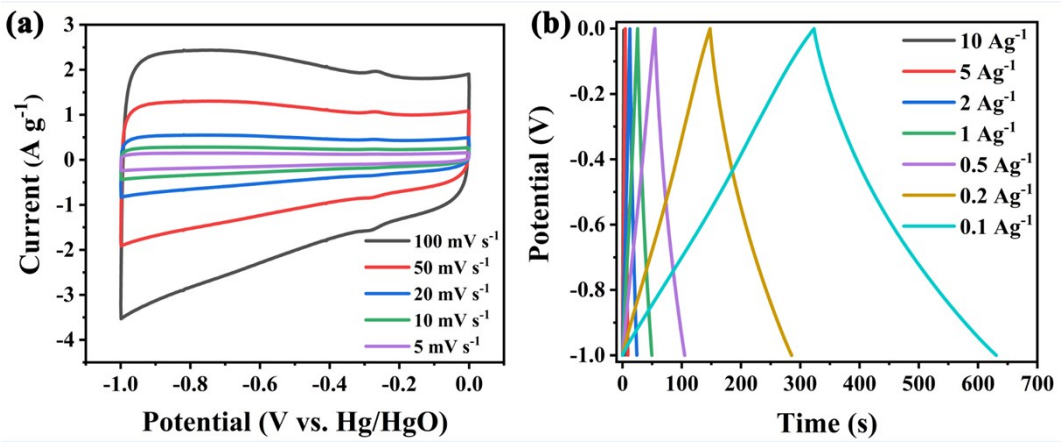

Figure S18. The CV and GCD curves at increasing scan rates and current density of the TiN.

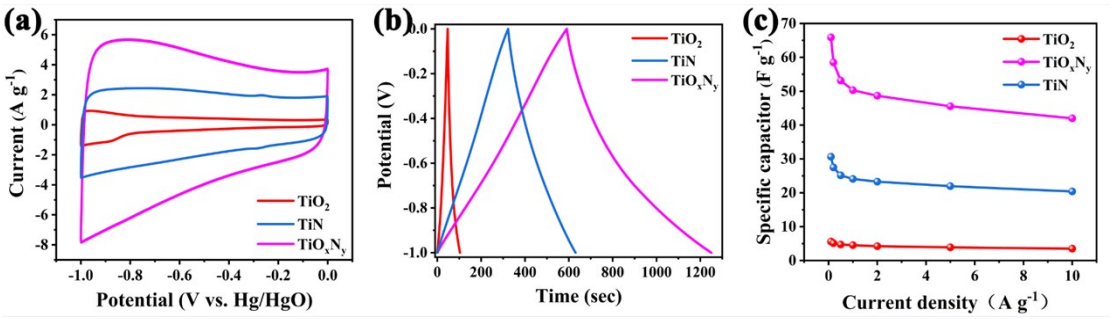

Figure S19. The CV, GCD and as a function of current density of the TiO_2, TiO_xN_y and TiN electrodes.

S6. Supplementary Table S1-S11

Table S1. The specific capacity at increasing current density of CM and CMM (M=Sn, Fe, V and Ti) electrodes.

Current density	0.1 A g^{-1}	0.2 A g^{-1}	0.5 A g^{-1}	1 A g^{-1}	2 A g^{-1}	5 A g^{-1}	10 A g^{-1}
SnO_2	13.35	11.00	9.68	9.13	8.54	8.00	7.40
SnO_xN_y	26.97	21.96	17.05	15.47	13.98	12.90	12.40
Multiple	2.02	2.00	1.76	1.69	1.64	1.61	1.68
Fe_2O_3	98.86	87.12	59.17	52.57	47.57	41.56	37.33
FeO_xN_y	193.34	162.08	133.31	118.11	105.33	89.89	77.22
Multiple	1.96	1.86	2.25	2.24	2.21	2.16	2.07
VO_2	68.24	55.08	45.01	39.40	36.00	34.05	33.20
VO_xN_y	459.72	358.14	304.29	286.56	275.66	266.41	261.68
Multiple	6.73	6.50	6.76	7.27	7.66	7.82	7.88
TiO_2	5.61	5.134	4.73	4.56	4.24	3.90	3.50
TiO_xN_y	65.90	58.50	53.15	50.30	48.66	45.55	42.00
Multiple	11.75	11.39	11.25	11.03	11.48	11.68	12.00

Table S2. Rs and Rct values of CM electrodes and CMM electrodes.

	SnO_2	SnON	Fe_2O_3	FeON	VO_2	VON	TiO_2	TiON	TiN
Rs (Ω)	0.68	0.65	0.61	0.58	0.51	0.49	0.61	0.59	0.44
Rct (Ω)	0.66	0.32	0.83	0.45	0.52	0.23	1.06	0.29	0.026

Table S3. Resistivity and conductivity of CM electrodes and CMM electrodes.

	L (cm)	S (cm^2)	R (Ω)	ρ (Ω□m^2□m^{-1})	σ (S□ m^{-1})
Fe_2O_3/CF	1.51	0.01768	1025.307	0.120049	8.329915
FeO_xN_y/CF	1.506	0.01855	358.3033	0.044134	22.65845
SnO_2/CF	1.512	0.01584	929.7187	0.097399	10.26704

SnO_xN_y/CF	1.511	0.01734	523.343	0.060058	16.65056
VO_2/CF	1.498	0.01716	1040.405	0.119181	8.390579
VO_xN_y/CF	1.495	0.01656	875.3968	0.096967	10.31278
TiO_2/CF	1.502	0.0189	1131.838	0.142422	7.021401
TiO_xN_y/CF	1.505	0.01925	247.5031	0.031657	31.58822

able S4. Dielectric constant and dielectric loss of NiO.

Frequency	D (mU)	Cp (pF)	d (mm)	A (mm^2)	ε_0	ε_r
1K Hz	420	0.255	1.37	1.37	$8.85*10^{-12}$	28.814
2K Hz	320	0.232	1.37	1.37	$8.85*10^{-12}$	26.215
5K Hz	290	0.213	1.37	1.37	$8.85*10^{-12}$	24.068
10K Hz	288	0.2	1.37	1.37	$8.85*10^{-12}$	22.599
20K Hz	248	0.182	1.37	1.37	$8.85*10^{-12}$	20.565
50K Hz	171	0.167	1.37	1.37	$8.85*10^{-12}$	18.870
100K Hz	133	0.154	1.37	1.37	$8.85*10^{-12}$	17.401
200K Hz	125	0.143	1.37	1.37	$8.85*10^{-12}$	16.158
500K Hz	141	0.133	1.37	1.37	$8.85*10^{-12}$	15.028
1M Hz	174	0.125	1.37	1.37	$8.85*10^{-12}$	14.124
2M Hz	206	0.12	1.37	1.37	$8.85*10^{-12}$	13.559
5M Hz	233	0.113	1.37	1.37	$8.85*10^{-12}$	12.768
10M Hz	235	0.107	1.37	1.37	$8.85*10^{-12}$	12.090
20M Hz	226	0.101	1.37	1.37	$8.85*10^{-12}$	11.412
50M Hz	200	0.097	1.37	1.37	$8.85*10^{-12}$	10.960
80M Hz	185	0.093	1.37	1.37	$8.85*10^{-12}$	10.508

Table S5. Dielectric constant and dielectric loss of SnO_2.

Frequency	D (mU)	Cp (pF)	d (mm)	A (mm^2)	ε_0	ε_r
1K Hz	257	0.511	0.85	1.37	$8.85*10^{-12}$	35.824
2K Hz	238	0.475	0.85	1.37	$8.85*10^{-12}$	33.300
5K Hz	214	0.437	0.85	1.37	$8.85*10^{-12}$	30.636
10K Hz	201	0.417	0.85	1.37	$8.85*10^{-12}$	29.234
20K Hz	188	0.383	0.85	1.37	$8.85*10^{-12}$	26.851
50K Hz	145	0.352	0.85	1.37	$8.85*10^{-12}$	24.677
100K Hz	122	0.316	0.85	1.37	$8.85*10^{-12}$	22.153
200K Hz	119	0.289	0.85	1.37	$8.85*10^{-12}$	20.261
500K Hz	120	0.275	0.85	1.37	$8.85*10^{-12}$	19.279
1M Hz	128	0.251	0.85	1.37	$8.85*10^{-12}$	17.597

2M Hz	133	0.24	0.85	1.37	8. 85*10^{-12}	16.825
5M Hz	163	0.222	0.85	1.37	8. 85*10^{-12}	15.564
10M Hz	182	0.207	0.85	1.37	8. 85*10^{-12}	14.512
20M Hz	206	0.194	0.85	1.37	8. 85*10^{-12}	13.601
50M Hz	180	0.183	0.85	1.37	8. 85*10^{-12}	12.829
80M Hz	162	0.18	0.85	1.37	8. 85*10^{-12}	12.619

Table S6. Dielectric constant and dielectric loss of Fe_2O_3.

Frequency	D (mU)	Cp (pF)	d (mm)	A (mm^2)	ε_0	ε_r
1K Hz	208	0.438	1.27	1.37	8. 85*10^{-12}	45.879
2K Hz	179	0.404	1.27	1.37	8. 85*10^{-12}	42.318
5K Hz	158	0.37	1.27	1.37	8. 85*10^{-12}	38.756
10K Hz	140	0.336	1.27	1.37	8. 85*10^{-12}	35.195
20K Hz	130	0.306	1.27	1.37	8. 85*10^{-12}	32.052
50K Hz	148	0.276	1.27	1.37	8. 85*10^{-12}	28.910
100K Hz	132	0.246	1.27	1.37	8. 85*10^{-12}	25.768
200K Hz	122	0.226	1.27	1.37	8. 85*10^{-12}	23.673
500K Hz	116	0.205	1.27	1.37	8. 85*10^{-12}	21.473
1M Hz	112	0.185	1.27	1.37	8. 85*10^{-12}	19.378
2M Hz	123	0.175	1.27	1.37	8. 85*10^{-12}	18.331
5M Hz	133	0.164	1.27	1.37	8. 85*10^{-12}	17.178
10M Hz	142	0.163	1.27	1.37	8. 85*10^{-12}	17.074
20M Hz	135	0.153	1.27	1.37	8. 85*10^{-12}	16.026
50M Hz	130	0.146	1.27	1.37	8. 85*10^{-12}	15.293
80M Hz	127	0.138	1.27	1.37	8. 85*10^{-12}	14.455

Table S7. Dielectric constant and dielectric loss of Co_3O_4.

Frequency	D (mU)	Cp (pF)	d (mm)	A (mm^2)	ε_0	ε_r
1K Hz	186	0.898	0.85	1.37	8. 85*10^{-12}	62.955
2K Hz	170	0.781	0.85	1.37	8. 85*10^{-12}	54.753
5K Hz	132	0.693	0.85	1.37	8. 85*10^{-12}	48.583
10K Hz	103	0.623	0.85	1.37	8. 85*10^{-12}	43.676
20K Hz	85	0.56	0.85	1.37	8. 85*10^{-12}	39.259
50K Hz	73	0.519	0.85	1.37	8. 85*10^{-12}	36.385
100K Hz	62	0.475	0.85	1.37	8. 85*10^{-12}	33.300
200K Hz	53	0.437	0.85	1.37	8. 85*10^{-12}	30.636
500K Hz	48	0.411	0.85	1.37	8. 85*10^{-12}	28.814

1M Hz	58	0.376	0.85	1.37	8. 85*10^{-12}	26.360
2M Hz	60	0.357	0.85	1.37	8. 85*10^{-12}	25.028
5M Hz	71	0.354	0.85	1.37	8. 85*10^{-12}	24.818
10M Hz	75	0.34	0.85	1.37	8. 85*10^{-12}	23.836
20M Hz	62	0.326	0.85	1.37	8. 85*10^{-12}	22.855
50M Hz	58	0.317	0.85	1.37	8. 85*10^{-12}	22.224
80M Hz	55	0.314	0.85	1.37	8. 85*10^{-12}	22.013

Table S8. Dielectric constant and dielectric loss of VO_2.

Frequency	D (mU)	Cp (pF)	d (mm)	A (mm^2)	ε_0	ε_r
1K Hz	102	1.692	0.75	1.37	8. 85*10^{-12}	104.6641
2K Hz	83	1.469	0.75	1.37	8. 85*10^{-12}	90.86973
5K Hz	70	1.307	0.75	1.37	8. 85*10^{-12}	80.84869
10K Hz	62	1.2	0.75	1.37	8. 85*10^{-12}	74.22987
20K Hz	57	1.138	0.75	1.37	8. 85*10^{-12}	70.39466
50K Hz	52	1.084	0.75	1.37	8. 85*10^{-12}	67.05431
100K Hz	48	1.035	0.75	1.37	8. 85*10^{-12}	64.02326
200K Hz	42	0.992	0.75	1.37	8. 85*10^{-12}	61.36336
500K Hz	43	0.958	0.75	1.37	8. 85*10^{-12}	59.26018
1M Hz	48	0.93	0.75	1.37	8. 85*10^{-12}	57.52815
2M Hz	50	0.907	0.75	1.37	8. 85*10^{-12}	56.10541
5M Hz	62	0.887	0.75	1.37	8. 85*10^{-12}	54.86824
10M Hz	75	0.864	0.75	1.37	8. 85*10^{-12}	53.4455
20M Hz	86	0.855	0.75	1.37	8. 85*10^{-12}	52.88878
50M Hz	73	0.84	0.75	1.37	8. 85*10^{-12}	51.96091
80M Hz	68	0.824	0.75	1.37	8. 85*10^{-12}	50.97117

Table S9. Dielectric constant and dielectric loss of TiO_2.

Frequency	D (mU)	Cp (pF)	d (mm)	A (mm^2)	ε_0	ε_r
1K Hz	88	1.486	1.06	1.37	8. 85*10^{-12}	129.915
2K Hz	72	1.356	1.06	1.37	8. 85*10^{-12}	118.550
5K Hz	64	1.242	1.06	1.37	8. 85*10^{-12}	108.583
10K Hz	51	1.137	1.06	1.37	8. 85*10^{-12}	99.404
20K Hz	42	1.05	1.06	1.37	8. 85*10^{-12}	91.798
50K Hz	36	0.982	1.06	1.37	8. 85*10^{-12}	85.853
100K Hz	32	0.92	1.06	1.37	8. 85*10^{-12}	80.432
200K Hz	28	0.877	1.06	1.37	8. 85*10^{-12}	76.673

500K Hz	36	0.835	1.06	1.37	8. 85*10^{-12}	73.001
1M Hz	45	0.811	1.06	1.37	8. 85*10^{-12}	70.903
2M Hz	53	0.782	1.06	1.37	8. 85*10^{-12}	68.367
5M Hz	60	0.759	1.06	1.37	8. 85*10^{-12}	66.357
10M Hz	64	0.737	1.06	1.37	8. 85*10^{-12}	64.433
20M Hz	75	0.718	1.06	1.37	8. 85*10^{-12}	62.772
50M Hz	61	0.7	1.06	1.37	8. 85*10^{-12}	61.198
80M Hz	55	0.687	1.06	1.37	8. 85*10^{-12}	60.062

Table S10. The specific capacitance at increasing current density of Fe_2O_3 and FeO_xN_y electrodes with different 'A' values.

Current density	0.5 A g^{-1}	1 A g^{-1}	2 A g^{-1}	5 A g^{-1}	10 A g^{-1}
Fe_2O_3-1	**48.73**	**43.07**	**38.96**	**34.02**	**30.65**
FeO_xN_y-1	**104.89**	**92.17**	**86.08**	**72.99**	**64.73**
Multiple	**2.15**	**2.14**	**2.21**	**2.15**	**2.11**
Fe_2O_3-2	**33.32**	**28.99**	**25.88**	**22.48**	**20.09**
FeO_xN_y-2	**97.3**	**84.04**	**79.03**	**64.66**	**58.06**
Multiple	**2.92**	**2.90**	**3.05**	**2.88**	**2.89**

Table S11. The specific capacitance at increasing current density of TiO_2 and TiO_xN_y electrodes with different 'd' values.

Current density	0.5 A g^{-1}	1 A g^{-1}	2 A g^{-1}	5 A g^{-1}	10 A g^{-1}
TiO_2-1	**4.50**	**4.33**	**4.00**	**3.55**	**3.10**
TiO_xN_y-1	**59.12**	**54.79**	**53.15**	**42.90**	**39.80**
Multiple	**13.13**	**12.65**	**13.29**	**12.08**	**13.84**
TiO_2-2	**6.35**	**5.84**	**5.47**	**4.58**	**4.00**
TiO_xN_y -2	**68.87**	**62.29**	**56.03**	**50.93**	**43.13**
Multiple	**10.85**	**10.67**	**10.24**	**11.12**	**10.78**